Optically-induced Photodarkening and Photocrystallization in Amorphous Ag-Sb-S Films Prepared by Three Deposition Techniques

T. Wagner[1], J. Gutwirth[1], T. Kohoutek[1], M. Krbal[1], P. Bezdicka[2], J. Pokorny[3], M. Vlcek[4], M. Frumar[1]
[1]University of Pardubice, Department of General and Inorganic Chemistry and Research Centre of University Pardubice, 53210 Pardubice, Czech Republic (CR)*
[2]Institute of Inorganic Chemistry, ASCR, 25068 Rez u Prahy, CR.
[3]Department of Dielectrics, Institute of Physics, ASCR, Na Slovance 2, 18221 Praha 8, CR.
[4]Joint Laboratory of Solid State Chemistry of UPa and Inst. Macromol. Chem., ASCR, 53210 Pardubice, CR.

ABSTRACT

The amorphous films of $Sb_{33}S_{67}$ and $Ag_x(Sb_{0.33}S_{0.67})_{100-x}$ composition, where x is between 0 and 25 at.% Ag, were prepared by different techniques, i.e. by vacuum evaporation, optically-induced silver dissolution into the binary Sb-S chalcogenides deposited by vacuum evaporation or by spin coating techniques. Ternary Ag-Sb-S amorphous films were also prepared directly by pulsed laser deposition. We have studied effect of silver content in the host materials and Ar^+ ion laser exposure on optical properties and structure of the films. The optically-induced crystallization and photodarkening was proved in studied films and their potential application in optical memories could be expected.

1. INTRODUCTION

Amorphous chalcogenide films (amorphous chalcogenides of Ge, As, Sb, Te, Ag, In and other elements, with binary or multinary elements compositions) have got many potential and current applications in microoptics, photonic crystals and optical memories [1]. Optical memories (OM) recording mechanism is an optically-induced reversible phase transition between amorphous and crystalline state or the reversible local change in the films composition [2]. Above glass transition temperature, T_g, when softening takes place, a higher mobility state initially induced by lone pair electron absorption provides the ability for atoms to move slightly at very high speed to establish the new configurations leading to either crystallization or returning to the amorphous state, depending on conditions. The rewritability of OM films is connected with existence of euthectic, stoichiometric and/or compositions from the edge of glass formation for different chalcogenide systems [3]. The high density optical memories based on recording into chalcogenide thin films are currently used in industrial dimension but search for new materials continues [4]. Preparation of good quality thin films with desired composition for OM has been challenge, especially for complicated compositions where classical deposition techniques (e.g. vacuum thermal evaporation) fail. This paper deals with the films of $Ag_x(Sb_{0.33}S_{0.67})_{100-x}$ composition, where x is between 0 and 25 at.% Ag. Amorphous chalcogenide thin films have been prepared in Ag-Sb-S systems using different techniques, i.e. an optically-induced silver dissolution [5] into the binary Sb-S chalcogenides prepared by thermal evaporation or by spin coating techniques. Ternary Ag-Sb-S chalcogenide films were also formed by direct-pulsed laser deposition. This paper is focused on evaluation of photo-darkening kinetics during Ar^+ ion laser exposure to the films prepared by different deposition techniques. Structure was compared between exposed and unexposed films.

2. EXPERIMENTAL PROCEDURES

The fragments of the bulk $Sb_{33}S_{67}$ glass were used for *vacuum evaporation* (VE) from quartz crucible to avoid any contamination of the prepared films. The films were prepared on silica glass substrates in a 1 x 10^{-4} Pa vacuum, at a rate of 10 $nm.s^{-1}$. The constant thickness of films was guaranteed by rotating substrate holders in planetary system. Thickness waw monitored during evaporation with a quartz crystal monitor. The thickness of the $Sb_{33}S_{67}$ films was approximately 800 nm.
Bulk $Sb_{33}S_{67}$ samples were also powdered and then dissolved in n-butylamine into homogeneous dark brown solution (concentration approx. c = 0.5 $mol.l^{-1}$). Then thin films with composition of $Sb_{33}S_{67}$ were prepared by *spin coating* (SC)

* Correspondence: Email: tomas.wagner@upce.cz, tel./fax: +420466037144.

from $Sb_{33}S_{67}$ n-butylamine solution at a spin speed 2000 rpm and duration 20 seconds. Spin-coated films were stabilized in a vacuum furnace by heating at 90 °C for 24 hours. The thickness of the $Sb_{33}S_{67}$ SC films was 240 nm.
Subsequently, constant thickness film (~10 nm) of silver was evaporated step-by-step on the top of the chalcogenide VE and SC films. Both VE and SC $Sb_{33}S_{67}$ films were photodoped by consecutive *optically-induced diffusion and dissolution* (OIDD) of thin silver films (~10 nm). It resulted in homogeneous films of very good optical quality. The OIDD was carried out by illuminating the samples to a 500 W tungsten lamp equipped with large Fresnel lens and IR-cut filter.
Pulsed laser deposition (PLD) by KrF laser (λ = 248 nm, I = 2 J.cm^{-2}, f = 20 Hz, E = 300 mJ/puls, Lambda Physics Compex 102) was used and thin films were deposited on silica glass substrates from bulk plane-parallel samples with composition of $AgSbS_2$.
Raman spectroscopy has been carried out in laser exposed and unexposed films and bulk samples. The Raman spectroscopy of unexposed films and bulk glass samples was performed on a Fourier Transformation (FT) Raman spectrometer (Bruker, model IFS/FRA 106; Nd-YAG laser, λ = 1064 nm, I = 50 mW, 100-500 scans, resolution = 4 cm^{-1}). The films were mechanically peeled from the substrates, and immediately pressed into aluminium targets for the Raman measurements.
The optical recording was tested by spot exposures using Ar^+ ion laser (λ = 514 nm, with laser beam intensity I = 89 W.cm^{-2}, diameter = 1.1 mm, time scale from 0.5 to 20 seconds) into VE, SC and PLD films of $Ag_x(Sb_{0.33}S_{0.67})_{100-x}$ composition. Kinetics of the films photo-darkening (photocrystallization) were studied by Schnellphotometer Karl Zeiss Jena with photomultiplier and optical system Opton.
Micro-Raman spectra were recorded in the exposed spots (Renishaw, model 1000 with multichannel detection, excitation Ar^+ ion laser, λ = 514 nm, I = 0.1 mW, 500 scans).
Laser exposed dots were observed by SEM Jeol JSM – 550 LV with analyser IXRF systems and detector Gresham Sirius. Accelerating voltage was 20 kV. The same aparatus was used for qualitative and quantitative energy dispersive analysis (EDX).
Micro X-ray diffraction of exposed and unexposed films was measured on difractometer PANalytical X´PertPRO with Co (Kα) X-ray lamp (U = 30 kV, I = 45 mA) and Fe β filter. Semiconductor detector X'celerator was used for detection. Primary optics was silica monocapilary (diameter d = 0.1 mm), secondary optics was Soller slits (0.04 rad). Measurement time of one sample was approx. 24 hours.

3. RESULTS

Films in $Ag_x (Sb_{0.33}S_{0.67})_{100-x}$ system were prepared using different deposition techniques. Their composition and final thickness are summarized in Table 1.

Table 1. Films prepared by different deposition techniques. Abbreviations meanings are: (VE) vacuum evaporation, (SC) spin-coating, (OIDD) optically-induced diffusion and dissolution and (PLD) pulsed laser deposition.

films deposition technique	composition [at.%]	thickness [nm]	spot laser exposure
VE	$Sb_{33}S_{67}$	805	Figs. 1, 3, 5, 6 (a)
VE + OIDD	$Ag_{8.5}$ $(Sb_{0.33}S_{0.67})_{91.5}$	770	Figs. 1, 3, 4, 5, 6 (b)
SC + OIDD	$Ag_{15.3}$ $(Sb_{0.33}S_{0.67})_{84.7}$	240	Figs. 1, 3 5, 6 (c)
PLD	$Ag_{25.6}$ $(Sb_{0.33}S_{0.67})_{74.4}$	760	Figs. 1, 3 5, 6 (d)

Deposited films were exposed by Ar^+ ion laser (λ = 514 nm) with laser beam intensity I = 89 W.cm^{-2} and laser beam diameter equal to 1.1 mm to induce optically structural changes in films. Optically-induced structural changes in films were characterized by increasing level of photodarkening in light-exposed spots. The exposed (dark) and unexposed (light) parts of the films, in the view of transmission optical microscopy, was compared on each film in Figure 1.
The photodarkening kinetics was measured by following optical transmission of photodarkened spots in dependence on Ar^+ ion laser exposure duration. The typical kinetics curves are for all studied films plotted in Figure 2.
Micro Raman spectra were recorded in unexposed and exposed parts (t_{exp} = 20 s) (Fig. 3) of all films displayed in Figure 1. The Raman spectrum proves characteristic photo-induced changes in all studied films after their Ar^+ion laser spot exposures (I = 89 W.cm^{-2}) as it is shown in Figure 3 (a – d). Micro Raman spectrometry was also used to acquire data in

different times of exposure of sample b (see Tab. 1). Raman bands development after different times of exposure can be seen in Figure 4.

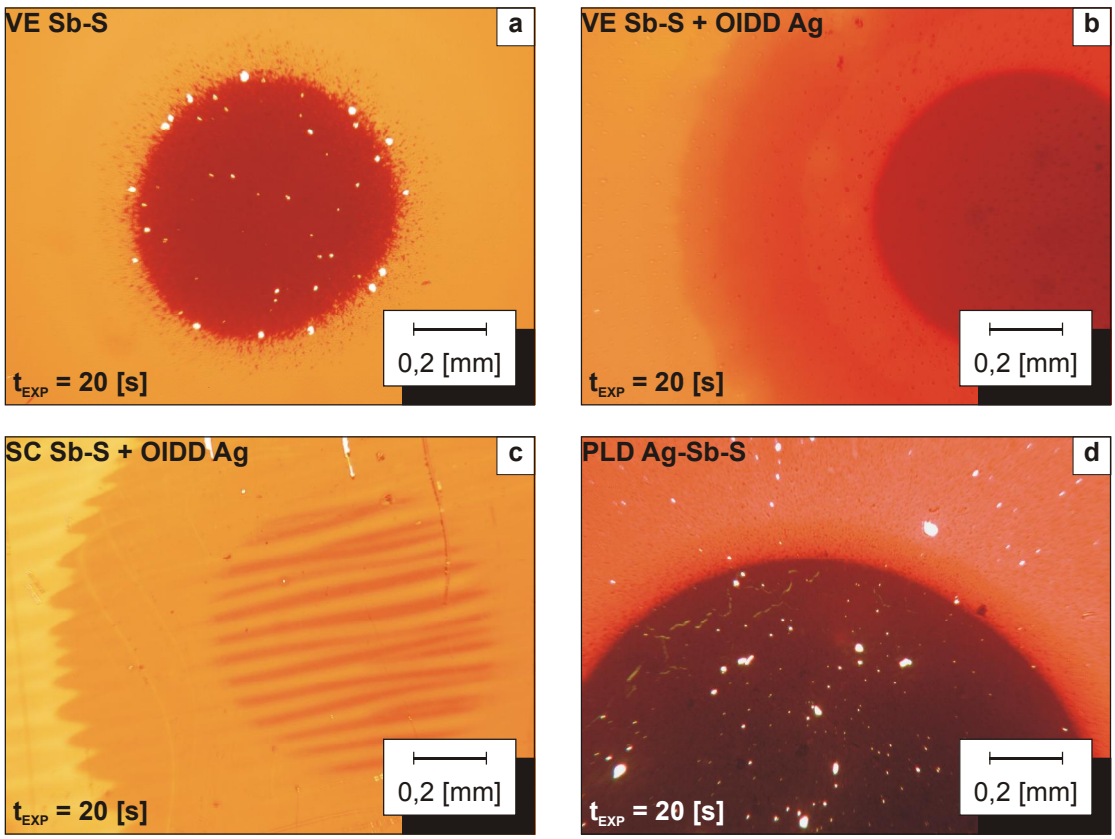

Fig. 1. The typical examples of Sb-S and Ag-Sb-S films with Ar^+ ion laser exposed spots. Each figure, (a) to (d) correspond to the sample in Table 1.

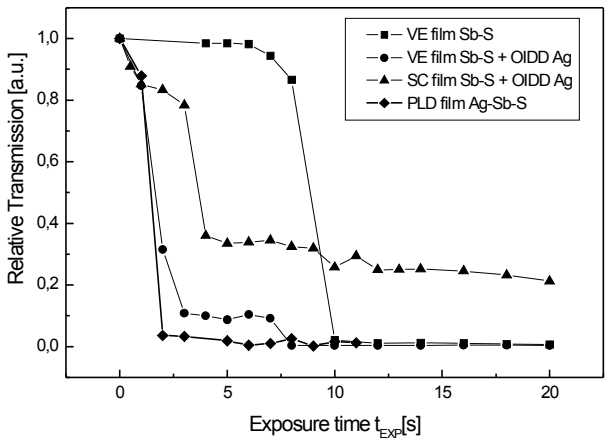

Fig. 2. Kinetics of photodarkening (photocrystallization) in all studied Sb-S and Ag-Sb-S films during exposure by Ar^+ ion laser with intensity I = 89 $W.cm^{-2}$.

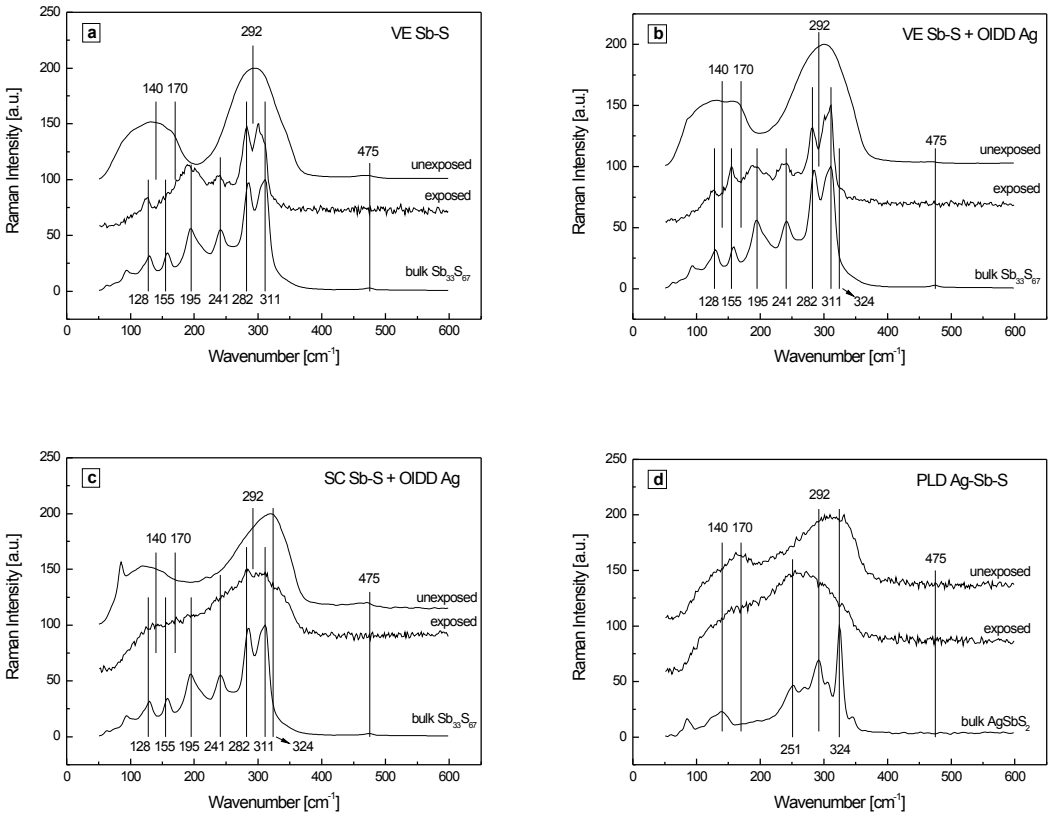

Fig. 3. Raman spectra measured in Ar^+ ion laser of exposed spots, unexposed films and bulks are shown for comparison. The assignment of each figure (a) to (d) corresponds to the sample description in Table 1.

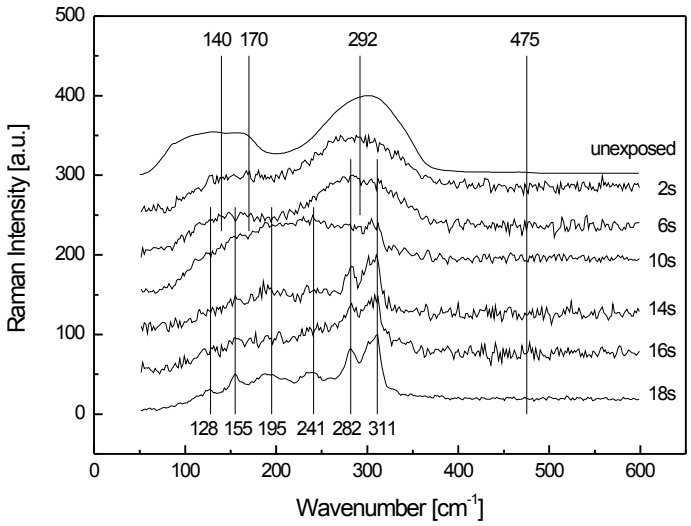

Fig. 4. Micro-Raman spectra obtained in Ar^+ ion laser exposed spots after different times of exposures of sample (b).

Optically-induced structural changes in films were also characterized by scanning electron microscopy (SEM) of Ar^+ ion laser exposed and unexposed part for all samples (a) to (d). The exposed and unexposed parts of the films, in the view of SEM was compared on each film in Figure 5.

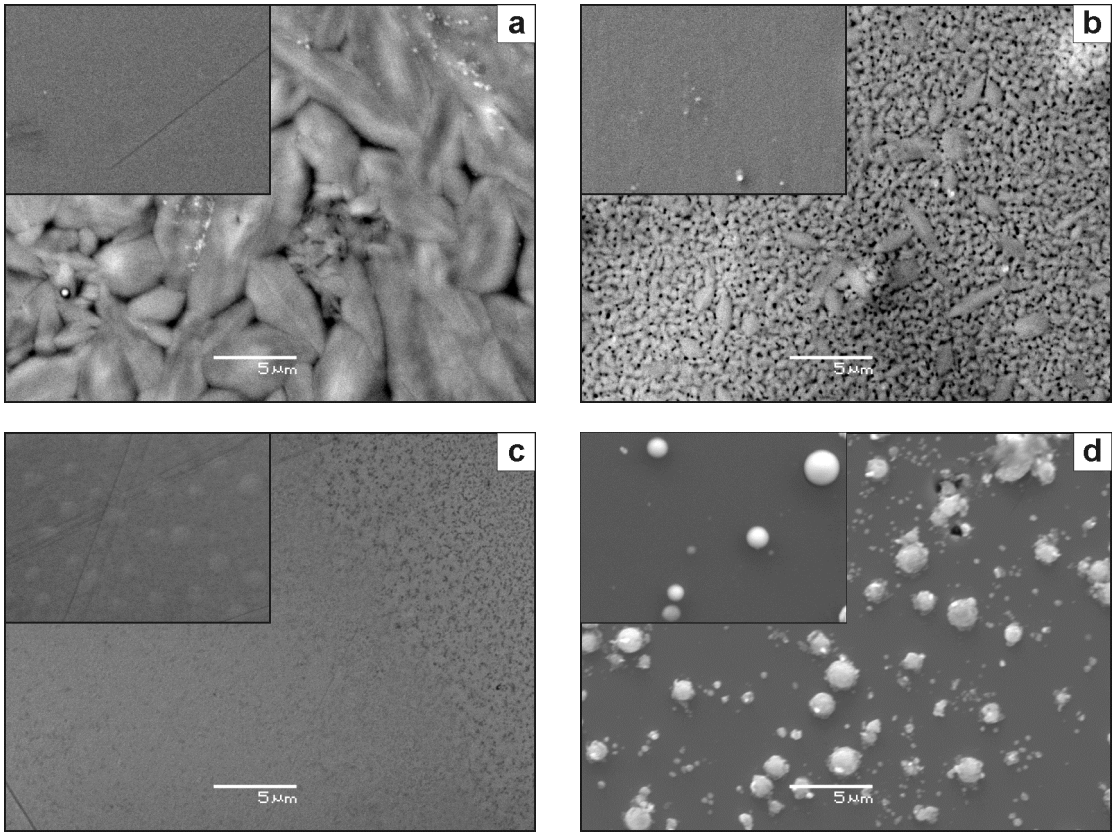

Fig. 5. Scanning electron microscopy of the unexposed (uper left insert in each figure) and exposed dots in prepared films. Each figure, (a) to (d) correspond to the sample (a) to (d) in Table 1.

Micro X-ray diffraction of Ar^+ ion laser exposed (20 sec) and unexposed dots for all samples (a) to (d) were recorded to study structural changes after laser exposure and the the characteristic diffractograms are shown in Figure 6.

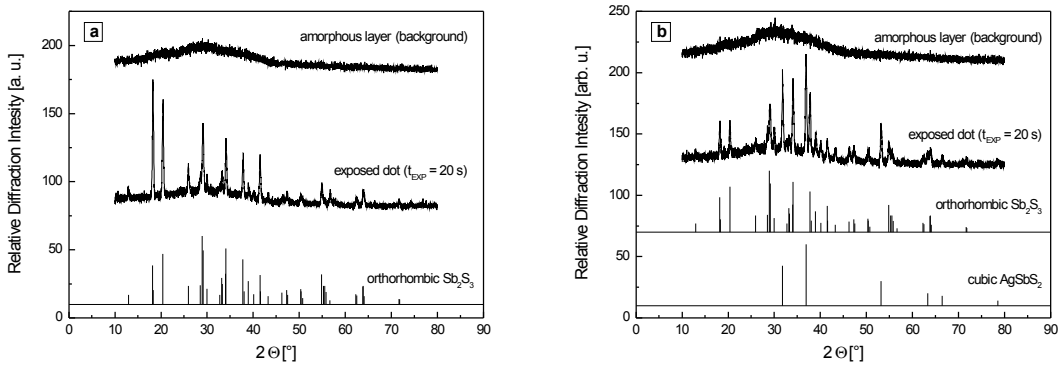

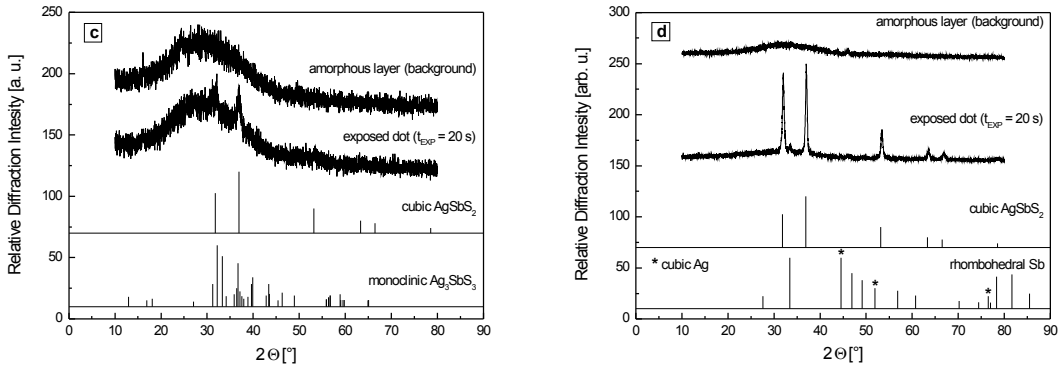

Fig. 6. Micro X-ray diffractogram of the unexposed (upper curve in each figure) and exposed dots of prepared films. Assignment of each figure (a) to (d) corresponds to the sample (a) to (d) in Table 1.

4. DISCUSSION

The aim of this work was to prepare amorphous films of Ag-Sb-S system including films with stoichiometric composition $AgSbS_2$. The $AgSbS_2$ stoichiometric compound has congruent melting and crystallization which allows faster recording process [6]. The different physico-chemical techniques allowed us to prepare films with different silver content. The silver content in films represents the concentration limit, which was possible to reach using the particular method (see Tab.1). The comparison of photodarkening (photocrystallization) kinetics measured in prepared (VE; VE SC and OIDD; PLD) films after laser exposure shows that the percolation time or abrupt change of optical density shifts to shorter time with increasing silver content in studied films in Fig. 2.

Raman spectra (Fig. 3 (a)-(d), upper curves) show unexposed films have amorphous character with typical broad band (324, 292, 170, 140 cm^{-1}) structure which could be assigned to the $SbS_{3/2}$ to $S_2Sb\text{-}SbS_2$ structural units vibrations according to Watanabe [7]. Raman spectra of Ar^+ ion laser exposed films with compositions $Sb_{33}S_{67}$ (VE) and $Ag_{8.5}(Sb_{0.33}S_{0.67})_{91.5}$ (VE+OIDD) taken in the saturation stage of photodarkening shows clearly the development of sharp bands (311, 282, 241, 195, 155, 128 cm^{-1}) (Fig. 3 a, b). Those bands could be assigned to Sb-S stretching and S-Sb-S bendings modes according to Minceva [8] Tab. 2. Raman bands sharpening in laser exposed films is also evidence of the simultaneous crystallization process. The evolution of the Raman bands at 311 and 282 cm^{-1} during Ar^+ ion laser exposure of sample (b) can be seen in Fig. 4 with notion that Raman spectroscopy can be also used to study the kinetics of crystallization in such films.

Table 2. The Raman frequencies, intensities and tentative assignment of the bands in Sb containing minerals [8].

Mineral	ν (Sb-S)	δ (S-Sb-S)
Stibnite, Sb_2S_3	443m 366w 291w 276w 247vs	184s 140s
Miargyrite, $AgSbS_2$	447m 370w 322vw 250vs	185s 134vw 115m

The Raman spectra (Fig. 3 (c), (d)) of the films with compositions $Ag_{15.3}(Sb_{0.33}S_{0.67})_{84.7}$ (SC+OIDD, sample (c)) and $Ag_{25.6}(Sb_{0.33}S_{0.67})_{74.4}$ (PLD, sample (d)) after laser exposure show broad band spectra with slight shift of bands to lower

frequencies without sharp distinct. Raman spectra of unexposed bulk samples with composition of $Sb_{33}S_{67}$ and $AgSbS_2$ are also presented for comparison in Fig. 3.
Scanning electron microscopy of studied sample allowed to see the surface structure and morphology of the films as it is shown in Fig. 5. Left upper corner of all the pictures belongs to unexposed part of the studied films. SEM of samples (a) and (b) clearly demonstrate crystallization process in films. The sample (c) does not visible crystallization within SEM resolution. The PLD sample (d) has visible surface deposits. Their origin is probably partly from pulsed laser deposition process and partly it could be effect of photo-induced surface silver deposition in Ag rich chalcogenide glasses described earlier by Kawaguchi [9].
XRD experiments performed for all samples as-deposited i.e. before Ar^+ ion laser exposure are amorphous (Fig. 6). XRD patterns of laser exposed films show lines corresponding crystalline phase as a result of exposure. Sample (a) in Fig. 6 was amorphous films with $Sb_{33}S_{67}$ composition which after exposure crystallizes in crystalline phase of orthorhombic Sb_2S_3. Sample (b) in Fig. 6 represents amorphous $Sb_{33}S_{67}$ films with 8 at.% of Ag. This amorphous films crystallizes after exposure and XRD peak belongs to orthorhombic Sb_2S_3 and cubic $AgSbS_2$. Sample (c) in Fig. 6 is amorphous $Sb_{33}S_{67}$ film prepared by spin-coating with 15 at.% of Ag. The film after exposure to Ar^+ ion laser crystallizes and XRD analysis proved existence of cubic crystals with composition of $AgSbS_2$ and probably traces (bellow 1%) of monoclinic phase Ag_3SbS_3. Sample (d) was prepared by pulsed laser deposition directly form the bulk material of $AgSbS_2$ composition. The Ar^+ ion laser exposure leads to crystallization of new phase containing cubic crystals with stoichiometric composition of $AgSbS_2$. There are probably present also minor traces of rhombohedral Sb and cubic Ag elements.

5. CONCLUSIONS

Binary Sb-S and ternary Ag-Sb-S films were prepared by vacuum evaporation, by spin coating method combined with optically induced silver diffusion and dissolution in Sb-S films and by pulsed laser deposition. Optical recording was performed by high power Ar^+ ion laser. Kinetics of photo darkening was characterized by percolation curve with abrupt transition shift to shorter exposition time with increasing silver content in films. Optically-induced structural changes in films after their exposure to Ar^+ ion laser were analyzed with help of Raman spectroscopy, which proved effects of photocrystallization in all samples. The crystallization products were orthorhombic Sb_2S_3 and cubic $AgSbS_2$.

ACKNOWLEDGEMENTS

Financial support from Grant Agency CR project no. 230/02/0087, from the Research Centre of University of Pardubice and Institute of Inorganic Chemistry ASCR, LN00A028 and IPHT Jena Germany (S. Schroeter) for laser exposure of samples.

REFERENCES

[1] P. J. S. Ewen, in: Photo-induced metastabilty in Amorphous (ed. A. V. Kolobov), Wiley-VCH, Weinheim, p. 365.
[2] T. Kawaguchi, in Photo-induced metastabilty in Amorphous (ed. A. V. Kolobov), Wiley-VCH, Weinheim, p. 182.
[3] R. S. Elliott, Physics of amorphous materials, Longman Scientific & Technical, Harlow, 1990, p. 57.
[4] T. Ohta and S. R. Ovshinski, in: in Photo-induced metastabilty in Amorphous (ed. A. V. Kolobov), Wiley-VCH, Weinheim, p. 310.
[5] M. Frumar and T. Wagner, Curr. Opin. Solid State Mater. Sci. 7 (2003) 117.
[6] I. Villars, A. Prince and H. Okamota, Handbook of Ternary Alloy Diagrams, vol. 3., ASM International, 1995, p. 2613.
[7] P. Watanabe, S. Noguchi, T. Shimizu, J. Non-Cryst. Solids 58 (1983) 35.
[8] B. Minceva-Sukarova, J. Mol. Struct. 651-653 (2003) 181.
[9] T. Kawaguchi and S. Maruno, J. Appl. Phys. 77 (1995) 628.